Settlement analysis of the Gloucester test fill

Lo, K. Y.; Bozozuk, M.; Law, K. T.

Publisher's version / Version de l'éditeur:
https://doi.org/10.4224/40000380
Paper (National Research Council of Canada. Division of Building Research), 1976

National Research Council Canada
Conseil national de recherches Canada

SETTLEMENT ANALYSIS OF THE GLOUCESTER TEST FILL

by K.Y. Lo, M. Bozozuk and K.T. Law

Reprinted from
Canadian Geotechnical Journal,
Vol. 13, 1976,
15p.

DBR Paper No. 691
Division of Building Research

Price 25 cents OTTAWA NRCC 15462

Canadian Geotechnical Journal

Revue canadienne de géotechnique

Published by
THE NATIONAL RESEARCH COUNCIL OF CANADA

Publiée par
LE CONSEIL NATIONAL DE RECHERCHES DU CANADA

Volume 13 Number 4 November 1976 Volume 13 numéro 4 novembre 1976

Settlement analysis of the Gloucester test fill

K. Y. LO
Faculty of Engineering Science, The University of Western Ontario, London, Ont., Canada N6A 3K7

AND

M. BOZOZUK AND K. T. LAW
Geotechnical Section, Division of Building Research, National Research Council of Canada, Ottawa, Ont., Canada K1A 0R6

Received April 18, 1975

Accepted May 26, 1976

This paper reports the observation and analysis of the rate and magnitude of settlement under the test embankment at Canadian Forces Station Gloucester. The embankment has been in existence for 7 years and, because of extensive instrumentation, a sufficiently complete record has emerged. An advanced finite element method has been used for the computation of the induced stresses in the foundation soil.

Both block samples and 5 in. (12.7 cm) diameter Osterberg samples were recovered at various depths from the site. An experimental program, including the use of the 6 in. (15.2 cm) Rowe cell, has been carried out and an analysis of the test results based on the Gibson and Lo theory. The test results have also been used in the estimation of the field performance.

From the present study it is found that: the coefficient of consolidation and the primary and secondary compressibility can be adequately determined from samples of size 4.5 in. (11.3 cm) diameter by 2 in. (5.1 cm) high or larger; the secondary compression contributes significantly to the total settlement for the soil considered; and the Gibson and Lo theory predicts fairly accurately both the time rate and magnitude of settlement in the field.

Cet article rend compte de l'observation et de l'analyse du taux et de la quantité de tassement du remblai d'essai de Base des Forces Canadiennes Gloucester. Grâce à une instrumentation considérable, le remblai en place depuis 7 ans, a fourni un dossier de données suffisamment complet. Une méthode avancée d'éléments finis fut utilisée pour le calcul des contraintes transmises dans le sol de fondation.

On a prélevé de différentes profondeurs des blocs d'échantillon et des échantillons au carottier Osterberg de 5 po. (12.7 cm) de diamètre. On a réalisé un programme d'essais, comprenant l'utilisation de la cellule Rowe de 6 po. (15.2 cm), et effectué l'analyse des résultats selon la théorie de Gibson et Lo. Les résultats d'essais ont également été utilisés pour l'estimation du comportement en chantier.

La présente étude démontre que: le coefficient de consolidation et la compressibilité primaire et secondaire peuvent être déterminés convenablement à l'aide d'échantillons de 4.5 po. (11.3 cm) de diamètre et 2 po. (5.1 cm) de hauteur ou plus gros; la compression secondaire contribue d'une manière significative au tassement total du sol considéré; la théorie de Gibson et Lo prédit avec suffisamment de précision le taux et la quantité du tassement en place.

[Traduit par la revue]

Can. Geotech. J., **13**, 339 (1976)

Introduction

In 1967, a test embankment was constructed and instrumented by the Division of Building Research, National Research Council of Canada at Canada Forces Station (C.F.S.) Gloucester, 13 mi (21 km) from Ottawa. The embankment, constructed in a 4 ft (1.2 m) deep excavation, is composed of a granular fill, 12 ft (3.7 m) high, 30 ft (9.2 m) wide, and 120 ft (36.6 m) long at the top, with 1.5 to 1 side slopes. The initial performance of the embankment has been described and analyzed by Bozozuk and Leonards (1972). Continuous monitoring of the test fill was maintained up to the end of 1974. From the results of these long-term observations, which covered a period of 7 years, it was found that most of the settlements, at the surface and at different depths of the subsoil, could be attributed to secondary compression. This case record is particularly significant in that pore water pressures, vertical settlements, and lateral movements were measured during this period so that both the nature of settlement and the geometric constraints under which they occurred could be clearly defined. The purpose of this paper is therefore (a) to present the results of long-term laboratory tests on specimens from block and tube samples, whereby the parameters governing primary and secondary compression are evaluated, and (b) to analyze and predict the long-term settlements using a theory of one-dimensional consolidation accounting for secondary compression (Gibson and Lo 1961).

Instrumentation

To measure the vertical, horizontal, and shear stresses transmitted to the subsoil, earth pressure gauges were installed at the base of the embankment. Vertical settlements at various locations were recorded with different settlement gauges, including one fluid settlement gauge used to obtain a continuous settlement profile along the base of the fill. Horizontal deformations were registered with gauge plates and inclinometers. Norwegian Geotechnical Institute piezometers with open standpipes were used for monitoring pore pressure response. The geometry of the embankment and the location of the instrumentation are shown in Fig. 1.

Subsoil Conditions

The soil profile and results of a detailed subsoil investigation are shown in Fig. 2. Based on *in situ* strength tests, the soil profile may be divided into three principal layers. The first, extending from the ground surface (elevation 261.5 ft or 79.7 m) to a depth of 23 ft (7.0 m), is further subdivided into strata A, B, C, and D, according to index properties. In this layer, the desiccated crust extends to a depth of 7.5 ft (2.3 m) and the strength increases from 210 psf (0.103 kg/cm^2) at this depth to 680 psf (0.332 kg/cm^2) at 23 ft (7.0 m). In the middle layer, from 23 to 43 ft (7.0 to 13.1 m) deep, the vane strengths increase from 460 to 980 psf (0.22 to 0.47 kg/cm^2). Underlying this formation from 43 to 60 ft (13.1 to 18.3 m), the strengths increase from 800 to 1080 psf (0.384 to 0.527 kg/cm^2). Finally, this formation is underlain with varved clay and glacial till. The *in situ* effective stress (from piezometric measurements) and the increase in vertical pressure under the centre of the test embankment are also shown. The average engineering properties of the soil are summarized in Table 1.

For this study, additional undisturbed 5 in. (12.7 cm) diameter Osterberg (1952) samples were taken 100 ft (33 m) west of the embankment to a depth of 50 ft (15.2 m), and block samples were recovered from a test trench adjacent to the test fill from a depth of 8 ft (2.4 m). The stress conditions at these locations were relatively unaffected by the embankment. Specimens were trimmed from both types of samples for laboratory tests.

Stress Increase Due to Embankment

In August 1967, the top part of the crust was excavated to a depth of 4 ft (1.2 m), over an area 94 ft (28.7 m) wide by 128 ft (39.0 m) long. The test fill was constructed on the floor of the excavation. Construction began 11 September, and by 6 October the test fill was level with the original ground surface. Construction was completed 13 October 1967. The net height of the embankment which was constructed in 1 week is 8 ft (2.4 m).

In this analysis, the stress changes due to embankment loading were computed using a

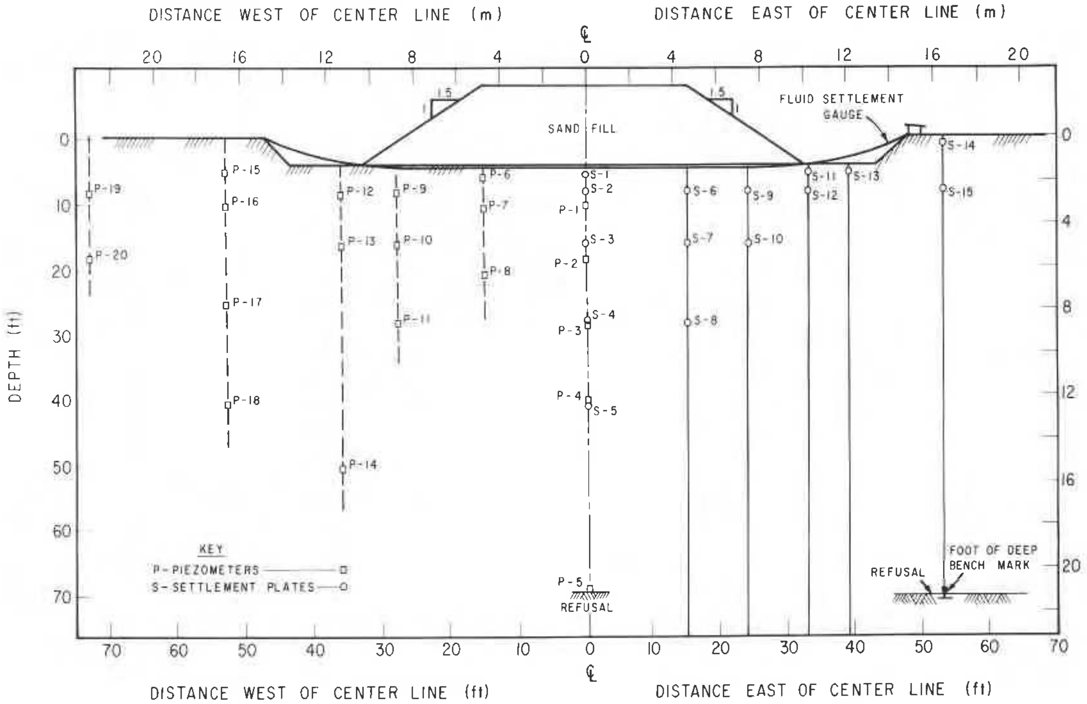

FIG. 1. Location of settlement gauges and piezometers.

finite element method incorporating the following conditions: (a) simulation of construction (excavation and backfilling) process in four steps, (b) taking into account embankment stiffness (and therefore induced shear stress along the embankment–soil interface) and stiff layer at 69 ft (21.1 m) depth, (c) using an average value of $K_0 = 0.75$ measured in the field by hydraulic fracturing method (Bozozuk 1974), and (d) the inhomogeneous distribution of undrained moduli E (Bozozuk 1972) was taken into account, and the undrained Poisson's ratio was taken as 0.49.

The stress–strain relationship in monotonically increasing loading of the sensitive clay was then assumed to be bilinear to represent a pseudo elasto-plastic behaviour, using the undrained strength profile based on *in situ* vane strength tests shown on Fig. 2. Further details of the method have been described elsewhere (Law and Lo 1976).

For these conditions, computations show that the increase in vertical stress is insensitive to the stress–strain relationship assumed. The applied stresses are compared with the *in situ* vertical effective stress and preconsolidation pressure on Fig. 2. The increase in vertical pressure $\Delta\sigma_z$ exceeds P_c to a depth of 17.5 ft (5.3 m) with the ratio of $\Delta p/(P_c - P_o) = 2.4$. Below 17.5 ft (5.3 m) the applied stresses are within the over-consolidated range. The ratio $\Delta p/(P_c - P_o)$ is about 0.67 from 17.5 ft (5.3 m) to 43 ft (13.2 m). Further down to bedrock $\Delta p/(P_c - P_o)$ is equal to 0.38. Along the base of the test embankment, the distribution of the normal (vertical and horizontal) and shear stresses determined by the finite element analysis compared favourably with the field measurements reported by Bozozuk and Leonards (1972).

Long-term Consolidation Tests

To study the consolidation behaviour of the clay strata, consolidation tests were carried out, (a) on specimens 2 in. (5.08 cm) in diameter and 0.5 in. (1.27 cm) thick, trimmed from 5 in. (12.7 cm) Osterberg samples taken at different depths (double drainage), (b) on specimens 2 in. (5.08 cm) in diameter and 0.5 in. (1.27 cm) thick, trimmed from block

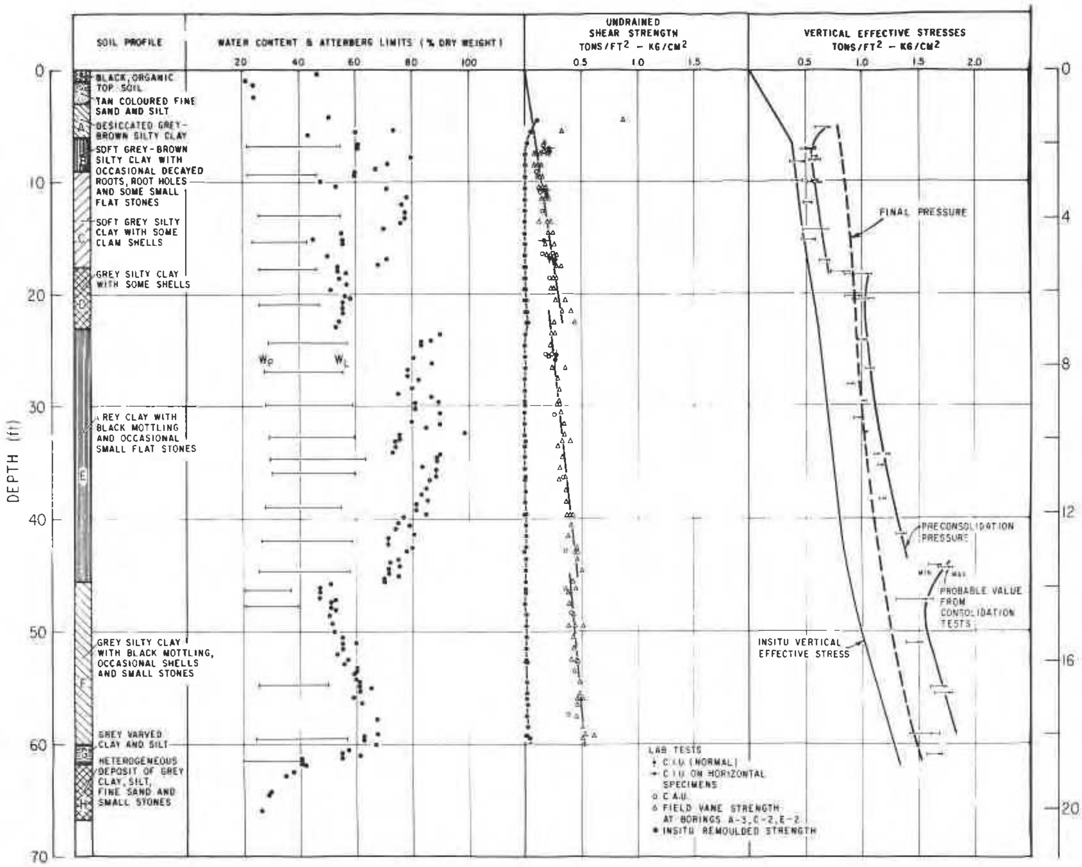

FIG. 2. Subsoil geotechnical profiles.

TABLE 1. Summary of index properties of soil at Gloucester test fill

Layer	Depth (ft)	W (%)	W_L (%)	PI (%)	LI	S_t	Activity	γ (pcf)	P_c/P_0
1	0–23	60	48	24	1.5	20–100	0.42–0.28	103	1.5
2	23–43	82	58	30	1.9	50–100	0.35	95	1.6
3	43–60	60	45	23	1.5	20–50	0.4	103	1.5

samples (double drainage), (c) on specimens 6 in. (15.24 cm) in diameter and 2 in. (5.08 cm) thick, trimmed from block samples (single drainage) using the Rowe cell and measuring the pore pressures at the base, and (d) on specimens 4.44 in. (11.28 cm) in diameter and 1.97 in. (5.0 cm) thick, trimmed from the Osterberg samples using a modified Rowe cell in which the axial load was applied by dead weights through a hanger system.

The samples were consolidated to the *in situ* vertical effective pressure for 3 days. Then a load corresponding to the stress increase beneath the centre line of the embankment was applied to correspond with the load increment ratio $\Delta p/p$ in the field. The important influence of the load increment ratio on consolidation behaviour has been discussed by Leonards and Girault (1961). In all tests, the time range of observation varied from 15 to 150 days.

The test results for the 2 in. (5.08 cm) diameter specimens are shown on Fig. 3, and for the 4.44 in. (11.28 cm) diameter and larger specimen on Fig. 4. The strange be-

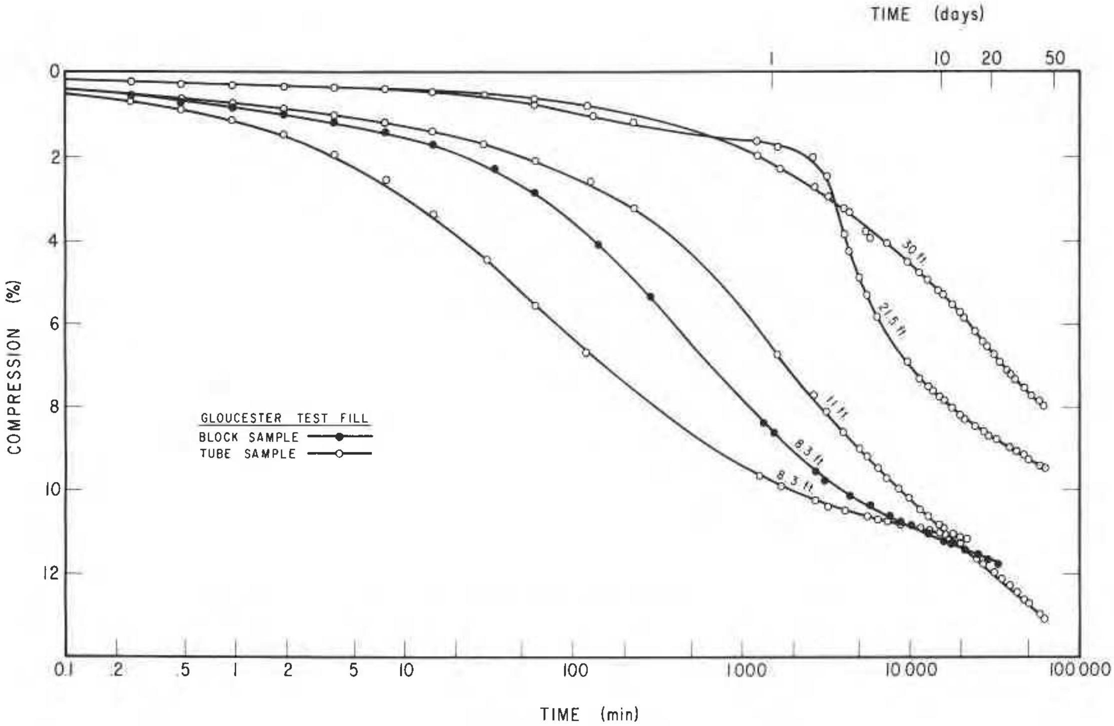

FIG. 3. Results of consolidation tests on 2 in. (5 cm) diameter specimens.

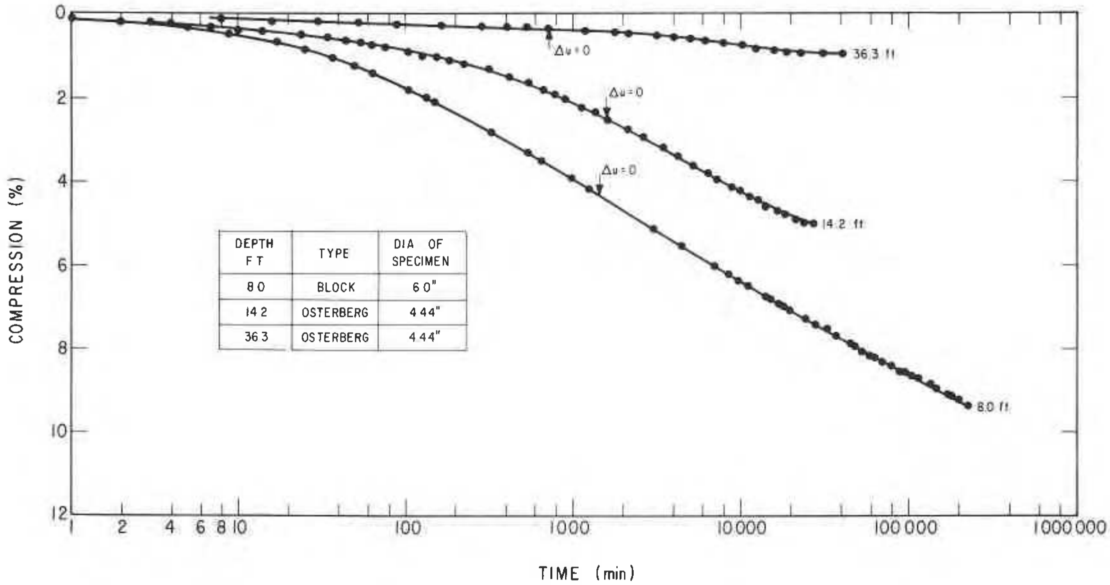

FIG. 4. Results of consolidation tests on 4.5 and 6 in. (11.4 and 15 cm) diameter specimens.

haviour of the specimen from 21.5 ft (6.56 m) was not due to experimental error as the results were reproducible even with a different test apparatus. It appears that the specimen resisted this stress level for a certain period of time. Beyond this point, the structure of the clay particles broke down, resulting in the increased rate of secondary compression with logarithm of time. Similar discussion was also given by Lo (1961). From the tests, the following general observations may be made:

(a) The pore pressure measured in the 6 in. × 2 in. (15.24 cm × 5.08 cm) specimen with single drainage (Fig. 4) shows that the average degree of 90% consolidation was reached in 350 min. This suggests that the corresponding time to reach the same degree of consolidation in the 2 in. × 0.5 in. (5.08 cm × 1.27 cm) sample with double drainage should be about 5.5 min. Based on conventional interpretation of test data (Fig. 3), however, a much longer period was obtained.

(b) A significant proportion of the total compression in most specimens (Figs. 3 and 4) was due to secondary compression.

(c) Few of the compression time curves show a linear relationship in the semi-log plot throughout the complete stage of secondary compression.

Methods of Predicting Settlement Due to Secondary Compression

Both empirical and theoretical methods have been developed for predicting settlements due to secondary compression. A common feature of the theories of consolidation taking secondary compression into account is that the time lag in secondary compression is attributed to the creep of the clay structure under constant effective stress. To incorporate this effect into the mathematical model the creep rate or viscous resistance has to be specified. In the empirical approach, a simple creep rate with respect to the logarithm of time is measured generally from oedometer tests (Buisman 1936; Leonards 1968; Walker and Raymond 1968). In the Gibson and Lo (1961) theory the structural viscosity is assumed to be linear. In the theories of Barden (1965) and Garlanger (1972), the viscosity is assumed to be nonlinear, with the result that the equations have to be solved numerically and the parameters cannot be precisely evaluated from experimental data. Since neither the mechanism of secondary compression nor the form of nonlinearity of the creep function is precisely known, it is preferable to retain the simplicity of a linear theory from which the parameters could be readily determined. The variation of these parameters may then be investigated and the nonlinearity studied. Nonlinear theories may then be adopted, if necessary. This approach is adopted in the evaluation of experimental results and analysis of field observations in this paper.

The Application of Gibson and Lo Theory

To describe the entire consolidation process, four soil parameters were used in this theory. The primary compressibility, a, governs that part of the soil compressibility due to dissipation of pore pressure. The secondary compressibility, b, governs the creep deformation under sustained effective stress. In addition to the time lag of pore pressure dissipation, compression of the clay is also retarded by the viscous deformation governed by the structural viscosity $1/\lambda$. The coefficient of consolidation c_v is defined in terms of the primary compressibility a and is equal to $k/(a\gamma_w)$, where k is the coefficient of permeability and γ_w the density of water.

With the same initial and boundary conditions as in the classical Terzaghi case, the expressions for pore presure u and average degree of consolidation $\bar{U}$ are given in the following dimensionless form (Gibson and Lo 1961):

$$[1]\quad \frac{u}{\Delta p} = \frac{4}{\pi} M \sum_{n=\text{odd}}^{\infty} \left[\bar{x}_1 \left(\frac{1}{M} - \frac{\bar{x}_2}{n^2\pi^2} \right) \times e^{-\bar{x}_2 T_1/4} - \bar{x}_2 \left(\frac{1}{M} - \frac{\bar{x}_1}{n^2\pi^2} \right) \times e^{-\bar{x}_1 T_1/4} \right] \frac{\sin \dfrac{n\pi z}{2h}}{n(\bar{x}_1 - \bar{x}_2)}$$

$$[2]\quad \bar{U} = 1 + \frac{8}{\pi^2} \sum_{n=\text{odd}}^{\infty} \left[\left(\frac{n^2\pi^2}{M} - \bar{x}_1 \right) e^{-\bar{x}_2 T_1/4} - \left(\frac{n^2\pi^2}{M} - \bar{x}_2 \right) e^{-\bar{x}_1 T_1/4} \right] \frac{1}{n^2(\bar{x}_1 - \bar{x}_2)}$$

where

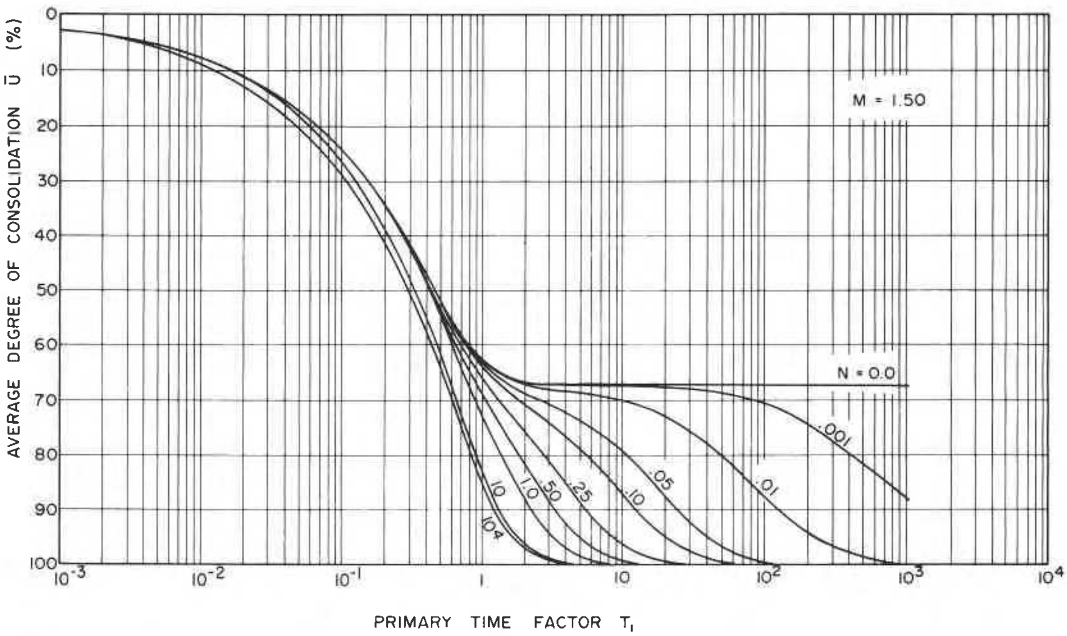

FIG. 5. Theoretical curves of average degree of consolidation ($M = 1.5$).

$$[3] \quad \left.\begin{matrix}\bar{x}_1 \\ \bar{x}_2\end{matrix}\right\} = \tfrac{1}{2}[(4MN + n^2\pi^2) \pm \{(4MN + n^2\pi^2)^2 - 16Nn^2\pi^2\}^{1/2}]$$

and

$$M = 1 + \frac{b}{a}$$

$$N = \frac{\lambda}{b}\frac{h^2}{c_v}, \quad h = \text{length of drainage path}$$

$$T_1 = \frac{c_v t}{h^2}$$

The settlement–time relationship can be computed from the equation:

$$[4] \qquad \rho(t) = \overline{U}(T_1)(a + b)\Delta\sigma_z' h$$

where $\rho(t)$ is the settlement at time t and $\Delta\sigma_z'$ the increase in effective vertical pressure.

Nomographs for pore pressure dissipation and average degree of consolidation *vs.* the time factor T_1 for different values of M and N are shown on Figs. 5 to 8. Many of these curves could be classified as Type II and III (Leonards and Ramiah 1959, Marsal *et al.* 1950) indicative of clays displaying high secondary compression. Note also that the 'waves' in the theoretical curves gradually smooth out as conditions proceed from the laboratory (N ranges from 0.001 to 0.01) to the field (N ranges from 0.1 to 1). The behaviour in the laboratory and in the field, however, is not simply related by the h or h^2 law. The functional relationship is complicated but is readily determined by choosing the appropriate theoretical curves for the corresponding N value in the field.

These parameters can be determined from long-term oedometer tests by the methods proposed by Gibson and Lo (1961). Another method that is particularly useful in the analysis of field records of settlement is described below.

A long time after the excess pore pressure has virtually dissipated, the approximate settlement $S(t)$ at any time t, is given by:

$$[5] \qquad S(t) = \Delta\sigma_z' h[a + b(1 - e^{(\lambda/b)t})]$$

The vertical strain $\epsilon(t)$ is given by the equation:

$$[6] \quad \epsilon(t) = \Delta\sigma_z'(a + b) - \Delta\sigma_z' be^{(-\lambda/b)t}$$

and the rate of secondary compression is:

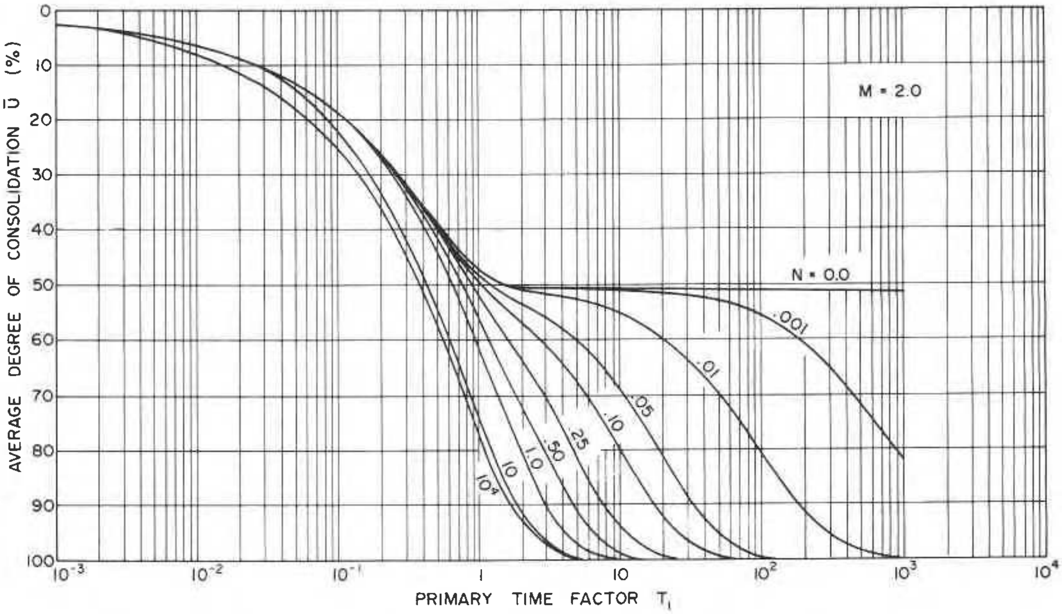

FIG. 6. Theoretical curves of average degree of consolidation ($M = 2.0$).

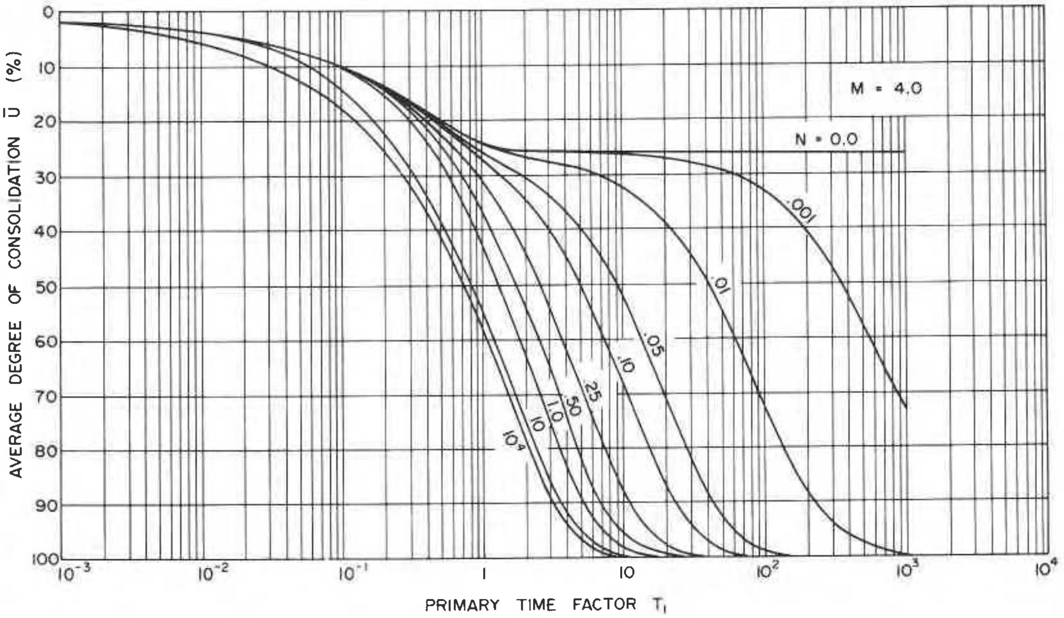

FIG. 7. Theoretical curves of average degree of consolidation ($M = 4.0$).

[7] $$\frac{\partial \epsilon(t)}{\partial t} = \Delta \sigma_z' \lambda \, e^{(-\lambda/b)t}$$

Taking the logarithm of both sides of [7]

[8] $$\log_{10} \frac{\partial \epsilon}{\partial t} = \log_{10} \Delta \sigma_z' \lambda - 0.434 \frac{\lambda}{b} t$$

Plotting the log of strain rate against time from laboratory or field results of a particular layer under consideration produces a straight line in the time range after excess pore pressures have dissipated. The slope of this line is given by $-0.434\ \lambda/b$, and the intercept yields

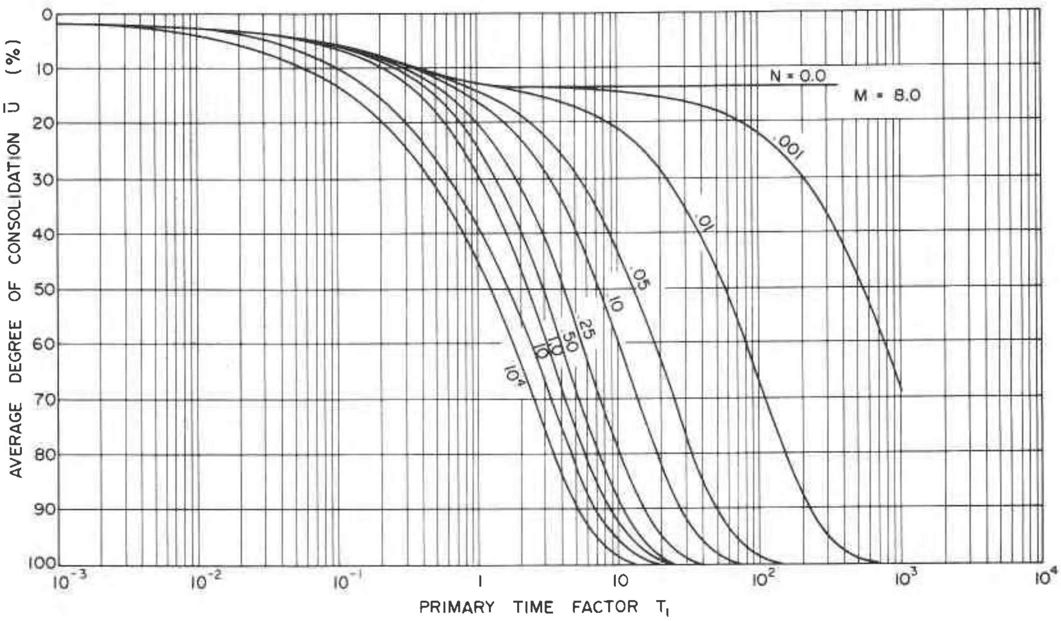

FIG. 8. Theoretical curves of average degree of consolidation ($M = 8.0$).

the value of $\log_{10}\Delta\sigma_z'\lambda$. Hence b and λ may be evaluated.

For a number of undisturbed and remoulded clays, linearity was obtained for a substantial time interval (Lo 1961). This suggests that the parameters are linear for the clays tested. Over a long period of time, however, (months in the laboratory and years in the field), there is no theoretical reason to believe that the parameters are strictly linear. It is known that the behaviour of some clays is sensitive to time or strain rate, and therefore, the parameter λ (or λ/b) may be highly dependent on time. Some evidence to this effect is discussed in the next section.

Analysis of Laboratory Test Results

The results from the test program described previously have been analyzed using [8]. Typical results for the 6 in. × 2 in. (15.24 cm × 5.08 cm) specimens are shown on Fig. 9. The curve can be approximated by a straight line in the time range from 3000 to 20 000 min, suggesting that the parameters b and λ are linear in this time range. The results of other tests, evaluated in the same way, are given in Table 2.

The most striking discrepancy between the results of the 4.44 in. × 2 in. (11.28 cm × 5.08 cm) or larger and the 2 in. × 0.5 in. (5.08 cm × 1.27 cm) samples lies in the vast difference in the coefficient of consolidation. The smaller samples yield c_v (Taylor 1948) one to two orders of magnitude less! The large decrease in c_v may be due to several important factors: (a) a larger proportion of sample disturbance resulting from trimming smaller samples (Van Zelst 1948; Bozozuk 1971); (b) larger hydraulic gradient due to shorter drainage path (1/8 that of larger sample); and, (c) larger strain rate in the earlier phase of consolidation (say from 0 to 1000 min). Temperature effects and mechanical disturbance from tube sampling may also play an important role. It is probable that the combination of factors (b) and (c) leads to a progressive destruction of the cementation bonds in sensitive clays, resulting in the erroneous low values of c_v. If such is the case, the primary compressibility a and b will also be in error when determined from the smaller specimens. Consequently, the test results from the larger samples are considered as representative. These are now being employed to study the nonlinearity of the parameters b and λ. Taking the instantaneous slope and intercept at a given time in Fig. 9, the parameters b and λ at any time may be calculated.

The results of calculations are plotted in Fig. 10. From this figure, it can be seen that b is

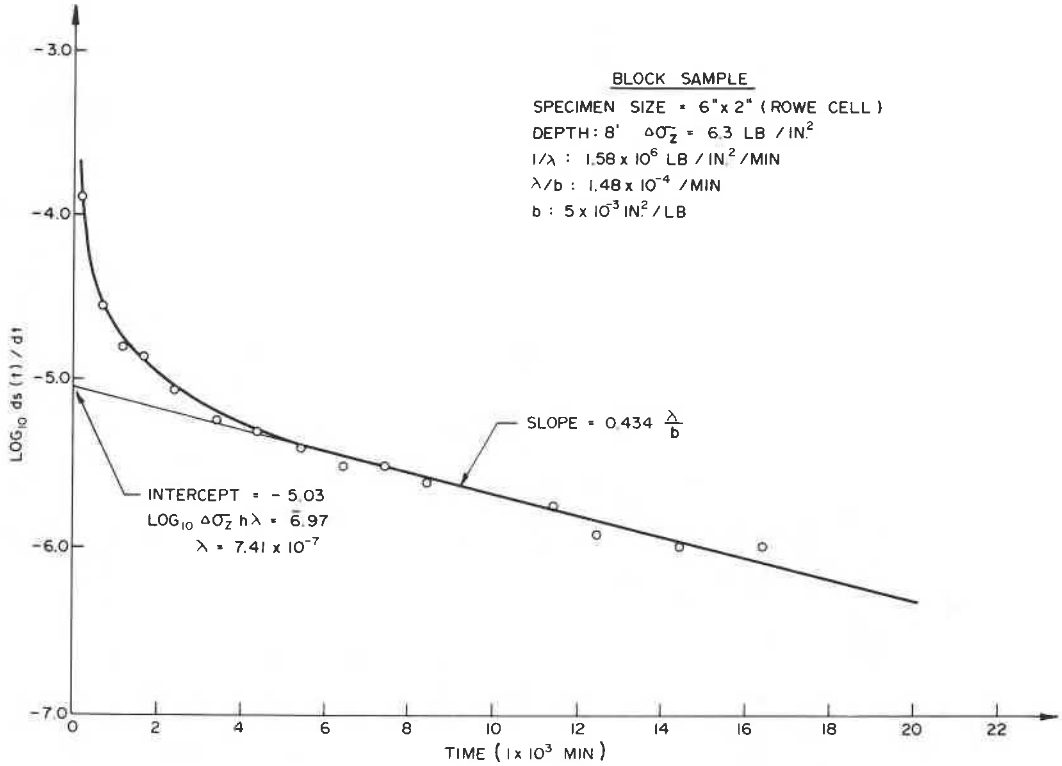

FIG. 9. Plot of log strain rate with time from laboratory tests.

relatively linear, a mildly nonlinear, and λ strongly nonlinear with time. For a satisfactory estimation of settlement in this particular record, both a and b were taken from the linear portion of the curve as shown in Fig. 9 while the value of λ has to be extrapolated to the range of time in the field. To enable proper extrapolation, the apparent hyperbolic shape of the curve (Fig. 10) is noted. In Fig. 11, log λ is therefore plotted against $1/\log t$. A linear trend is seen from test results on soil specimens recovered from the top compressible layer. For the other soil specimen from 36 ft (11 m) depth, a similar linear trend is observed after reaching a certain critical strain. Extrapolation to field time is then based upon this plot and the results, together with other parameters for estimating the long-term settlement, are shown in Table 3.

Analysis of Long-term Settlement

The field measurements of pore pressures and settlements at different depths beneath the centre line of the test embankment are shown in Figs. 12 and 13 respectively. Because of the seasonal fluctuation of the ground water table, direct interpretation of the pore pressure conditions from Fig. 12 is difficult. By comparing these pore pressures with those measured with four reference piezometers installed 100 ft (30.5 m) north of the embankment, it was found that a small excess head persisted from $1\frac{1}{2}$ years after construction to November 1974. The values of these residual pore pressures for P_1, P_2, P_3, and P_4 are 0.3, 0.7, 0.8, and 0.5 psi (0.02, 0.05, 0.06, and 0.035 kg/cm^2) respectively.

These measurements show that primary consolidation was largely completed $1\frac{1}{2}$ years after the full load was applied, and that subsequent settlement could be attributed mainly to secondary compression. Figure 13 also shows that a large proportion of settlements at different depths is due to secondary compression. The end of primary consolidation cannot be defined easily by conventional empirical procedure, and difficulty may arise in the use of the secondary coefficient c_α (Buisman 1936).

TABLE 2. Summary of results of long-term oedometer tests

Sample type	Sample size (in.)	Depth (ft)	W_l (%)	P_c (TSF)	Pressure increment (TSF)	$\Delta p/p$	c_v (ft^2/yr)	a (in.^{2}/lb $\times 10^{-3}$)	b (in.^{2}/lb $\times 10^{-3}$)	λ (in.^{2}/lb-min $\times 10^{-7}$)
Block	6 × 2	8	66.1	0.58	0.40–0.84 (0.44)	1.1	29.6 51.0*	6.3	5.0	6.25
Block	2 × 0.5	8	67.0	0.58	0.40–0.84 (0.44)	1.1	0.29	14.0	4.0	2.22
Tube	2 × 0.5	8.3	56.3	0.58	0.40–0.84 (0.44)	1.1	3.04	16.0	2.0	0.68
Tube	2 × 0.5	11.0	87.0	0.60	0.43–0.84 (0.41)	0.95	0.48	15.3	7.7	1.0
Tube	2 × 0.5	21.5	75.7	1.0	0.58–0.86 (0.28)	0.47	χ†	5.0	19.0	2.5
Tube	2 × 0.5	30.0	86.0	1.1	0.68–0.96 (0.28)	0.41	χ	9.0	12.0	1.0
Osterberg	4.5 × 2	14.2	70.6	0.65	0.45–0.86 (0.41)	0.91	28.7	5.18	4.17	2.89
Osterberg	4.5 × 2	36.3	87.0	1.20	0.76–1.04 (0.28)	0.37	27.9	1.01	1.39	1.65

*From dissipation of pore water pressure.
†χ = curves that are inappropriate to determine c_v.

TABLE 3. Summary of soil parameters for estimating long-term settlement

Layer No.	Layer thickness (ft)	$\Delta\sigma_z$ (psi)	a (in.^{2}/lb $\times 10^{-3}$)	b (in.^{2}/lb $\times 10^{-3}$)	λ (in.^{2}/lb-min $\times 10^{-9}$)	k* (ft/min $\times 10^{-7}$)	c_v† (ft^2/yr)	Remarks
1	2.9	6.3	6.3	5.0	6.0	1.64	31.5	Single drainage
2	8.2	5.9	5.18	4.17	6.0	1.64	38.4	Single drainage
3	54.0	4.0	1.01	1.39	0.035	1.31	157.3	Double drainage

*From field tests (Bozozuk 1972).
†From $c_v = k/a\gamma_w$.

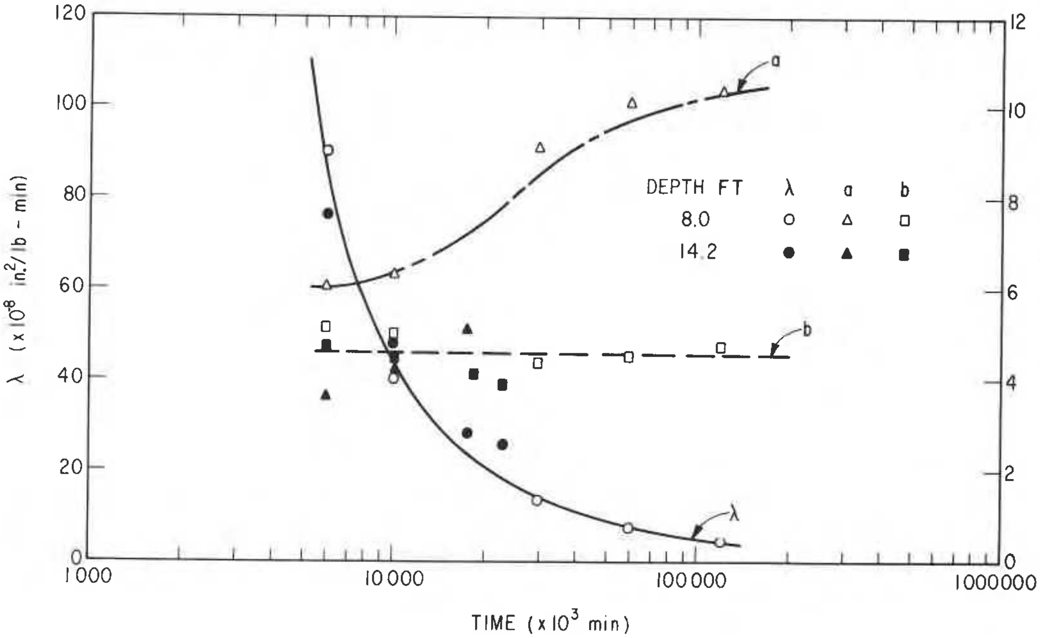

FIG. 10. Variations of parameters λ, a, and b with time from 4.5 and 6 in. (11.4 and 15 cm) diameter samples.

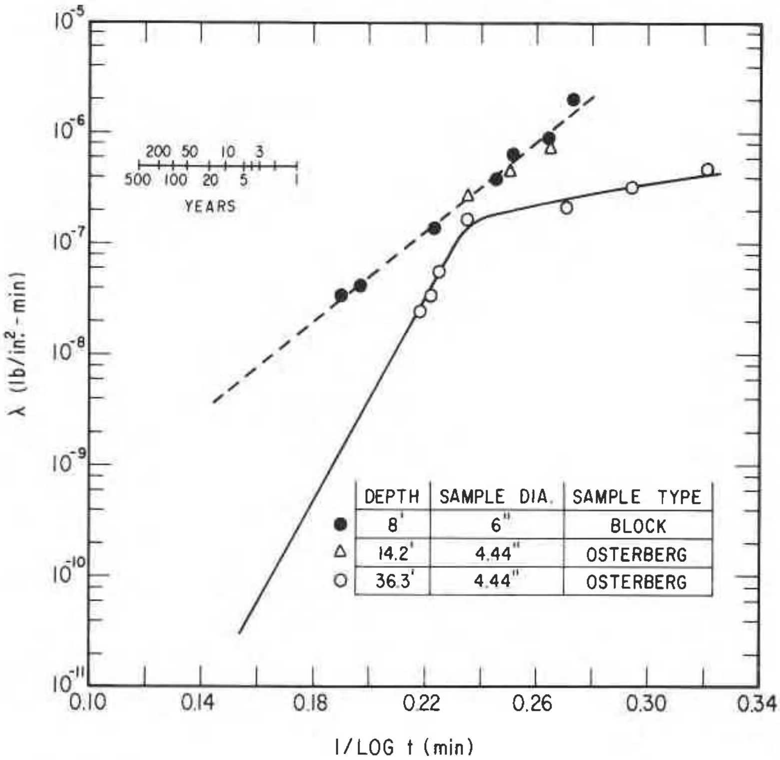

FIG. 11. Variation of λ with time.

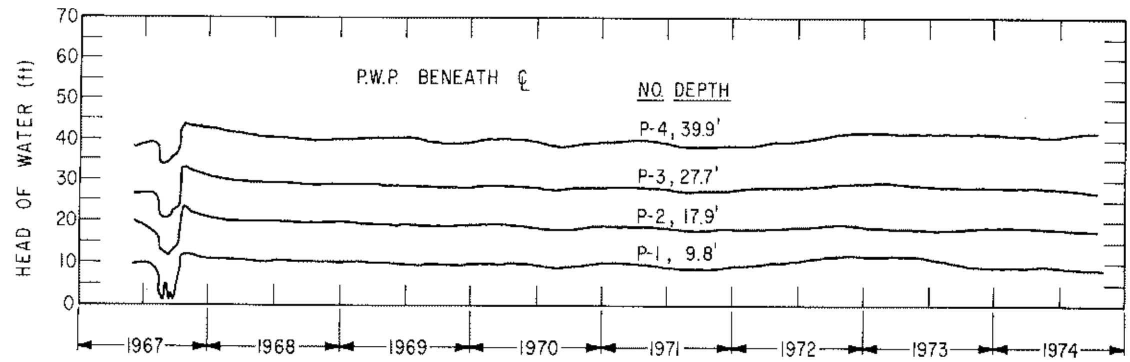

FIG. 12. Pore pressure record along centre line.

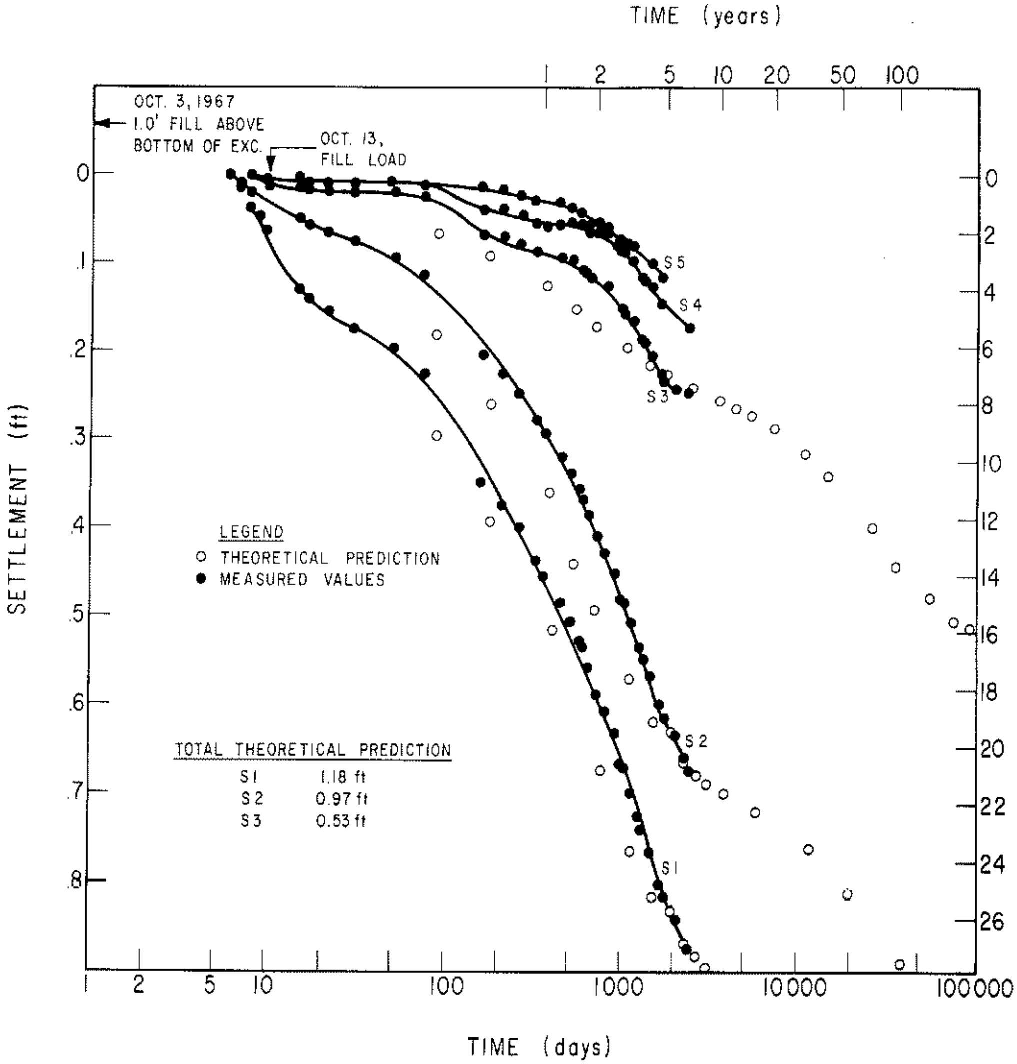

FIG. 13. Predicted and observed settlement along centre line.

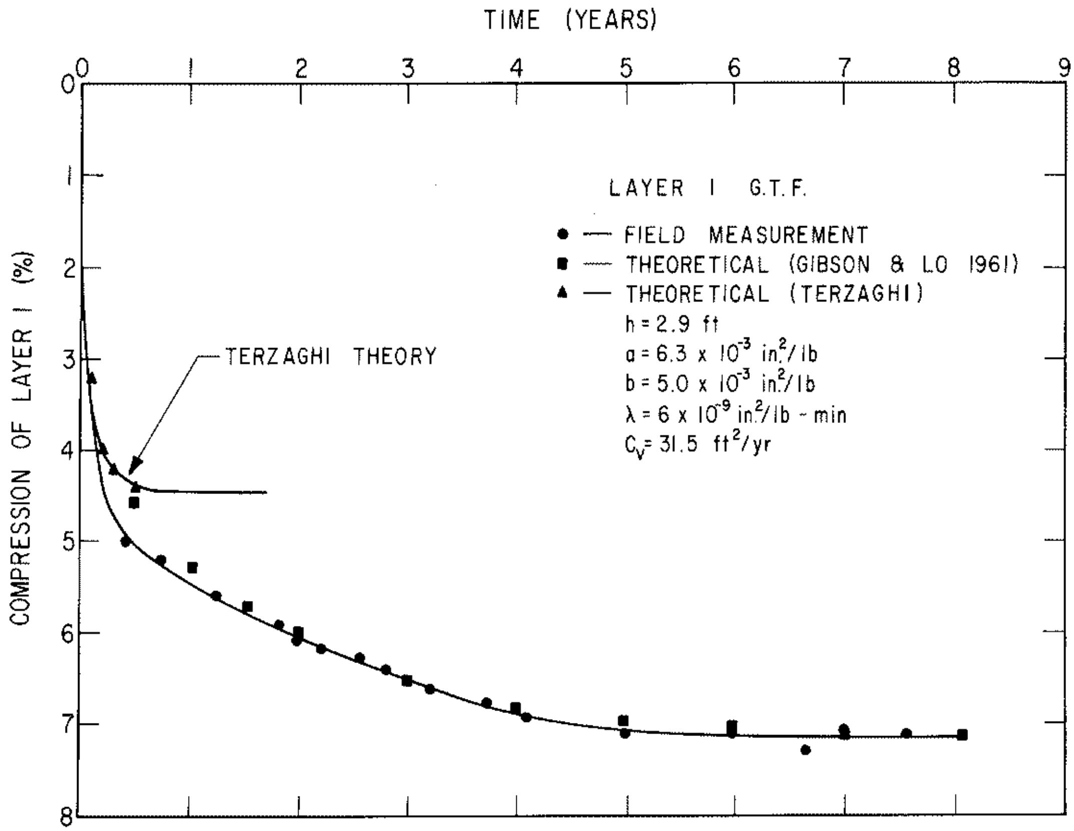

FIG. 14. Predicted and observed compression of the top layer of soil (layer 1).

To analyze the long-term settlements shown in Fig. 13, the entire deposit was divided into three layers in accordance with the location of measurements at different depths: layer 1 between plates S1 and S2; layer 2 between S2 and S3; and layer 3 between S3 and bottom of the deposit. The reason for considering the soil below S3 as one layer is that settlements recorded by S4 are too small for an accurate analysis. Data for the analysis are given in Table 3.

Comparison of Theoretical and Measured Settlement–Time Curve of Layer 1

The comparison of predicted consolidation of layer 1 with the field measurements is shown in Fig. 14. The agreement is reasonable both in magnitude and time rate of settlement. In the same figure is also plotted the estimated settlement based on Terzaghi's theory (1944). Using data obtained from 24 h tests, the classical Terzaghi's theory considerably underestimates the measured settlement.

Long Term Settlements of the Foundation Clay

Figure 13 shows the predicted and measured settlement at the elevations of the different settlement gauges. The general agreement is satisfactory. The somewhat larger predicted settlement stems from a slightly higher computed compression in the third layer. This is probably caused by an over-estimated value of a obtained from the laboratory test on the Osterberg sample. This over-estimation is particularly true since the loading intensity in layer 3 is below the preconsolidation pressure (Lo 1972).

The distributions of predicted and measured settlements along the centre line in the foundation clay at various times of interest is depicted in Fig. 15. Good agreement can be seen in the general shape of settlement profiles at different times.

Discussion

The present approach involved the use of a one-dimensional (1-D) model for the approxi-

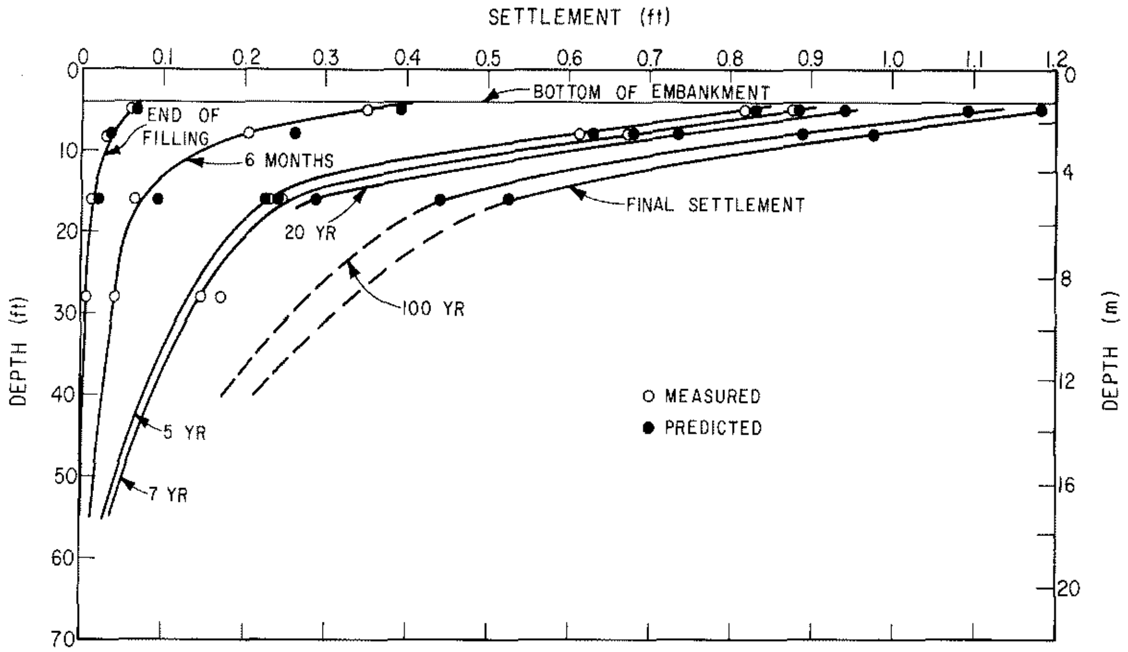

FIG. 15. Predicted and measured settlements at various times.

mate solution of a two-dimensional (2-D) problem. The apparent success of the method is based upon the following.

1. Test data from high quality (block and Osterberg) samples tested in a large Rowe cell were employed in the analysis.

2. By dividing the subsoil into three layers, the average induced vertical pressures in each layer have been used in conducting the laboratory tests and in estimating the settlement. Such a separation allows the treatment of that aspect of the 2-D effect, which induces a steadily decreasing change in vertical pressure with depth.

3. The effect of lateral drainage and horizontal displacement may not be significant in the first two layers where the ratio of width of loaded area to thickness of soil layer exceeds 2. There may, however, be a larger discrepancy in the third layer. This effect is not serious as this layer is far less compressible than the upper ones.

The use of the present approach should therefore be confined to cases similar to the one presented. In view of the good agreement, however, further verification of this approach is warranted.

Conclusions

Predicted and observed long-term settlement of the Gloucester test fill are presented. Consolidation tests to define the parameters governing both primary and secondary compression have been performed on specimens trimmed from block and tube samples taken from this site. The results were analyzed by a theory of consolidation accounting for secondary compression and the predicted long-term settlements were compared with field measurements. The conclusions resulting from this study may be summarized as follows:

1. Reasonable estimates of the coefficient of consolidation, c_v, the primary compressibility, a, and the secondary compressibility, b, may be obtained from long-term consolidation tests on specimens 4.5 in. (11.3 cm) diameter by 2 in. (5.0 cm) high or larger with pore pressure measurements.

2. The structural viscosity $1/\lambda$ or its reciprocal, λ, is strongly nonlinear with time. To apply the laboratory results to the field, λ must be extrapolated to the field time.

3. The field measurements indicate that a large proportion of the settlements at different depths are attributable to secondary compression occurring at essentially constant effective stress.

4. The application of Gibson and Lo's theory results in reasonable agreement in time

rate and magnitude of settlement along the centre line of the embankment.

Acknowledgement

The authors gratefully acknowledge the co-operation of the Ontario Ministry of Transportation and Communications (OMTC) and thank them for their permission to publish these research results. The work performed is part of a project supported by the OMTC under the Ontario Joint Transportation and Communications Research Program. It is also part of a co-operative study of the Division of Building Research, National Research Council of Canada, and the Faculty of Engineering Science, University of Western Ontario.

This paper is a contribution from the Division of Building Research, National Research Council of Canada, and is published with the approval of the Director of the Division.

BARDEN, L. 1965. Consolidation of clay with non-linear viscosity. Geotechnique, **15**(4), pp. 345–362.

BOZOZUK, M. 1971. Effect of sampling, size, and storage on test results for marine clay. Am. Soc. Test. Mater. Spec. Tech. Publ. No. 483, pp. 121–131.

——— 1972. The Gloucester test fill. Unpubl. PhD thesis, Purdue Univ., Lafayette, Ind.

——— 1974. Minor principal stress measurement in marine clay with hydraulic fracture tests. Subsurface exploration for underground exploration and heavy construction. Proc. Spec. Conf., New England College, Henniker, N.H., August 11–16, 1974. pp. 333–349.

BOZOZUK, M. and LEONARDS, G. A. 1972. The Gloucester test fill. Spec. Conf. on Performance of Earth and Earth-Supported Structures, ASCE, Purdue Univ. Lafayette, Ind., vol. 1, part 1, pp. 299–317.

BUISMAN, A. S. K. 1936. Results of long duration settlement tests. Proc. 1st Int. Conf. on Soil Mechanics and Foundation Engineering, Cambridge, Mass., vol. 1, pp. 103–105.

GARLANGER, J. E. 1972. The consolidation of soils exhibiting creep under constant effective stress. Geotechnique, **22**(1), pp. 71–78.

GIBSON, R. E. and LO, K. Y. 1961. A theory of consolidation of soils exhibiting secondary compression. Acta Polytechnical Scandinavia, Ci 10 296 (Scandinavian Academy of Science).

LAW, K. T. and LO, K. Y. 1976. Analysis of shear-induced anisotropy in Leda Clay. Proc., 2nd Int. Conf. on Numerical Methods in Geomechanics. Blacksburg, Va., vol. 1, pp. 329–344.

LEONARDS, G. A. 1968. Predicting settlements of buildings on clay soils. Proc. Lecture series January – May, 1968, Ill. section ASCE, Northwestern Univ., Evanston, Ill.

LEONARDS, G. A. and GIRAULT, P. 1961. A study of the one-dimensional consolidation test. Proc. 5th Int. Conf. on Soil Mechanics and Foundation Engineering, Paris, France, vol. 1, pp. 213–218.

LEONARDS, G. A. and RAMIAH, B. K. 1959. Time effects in the consolidation of clays. Symp. on Time Rate of Loading in Testing Soils, Am. Soc. Test. Mater. Spec. Tech. Publ. No. 254, pp. 116–130.

LO, K. Y. 1961. Secondary compression of clays. ASCE, J. Soil Mech. Found. Div. **87**(SM4), pp. 61–87.

——— 1972. The influence of mechanical disturbance on the consolidation of clays. 3rd Proc. Southeast Asian Conf. on Soil Engineering. pp. 223–232.

MARSAL, R. J., SANDOVAL, R., and HIRIAT, F. 1950. Curvas deformacion-tiempo en las arcillas del Valle de Mexico (Time–deformation curves in clays from the valley of Mexico). Ingenieria civil, colegio de Ingenieria Civiles de Mexico, **2**(5), pp. 7–17.

OSTERBERG, J. O. 1952. New piston tube sampler. Eng. News-Rec. **148**, pp. 77–78.

TAYLOR, D. W. 1948. Fundamentals of Soil Mechanics. John Wiley and Sons, Inc., New York, N.Y.

TERZAGHI, K. 1944. Theoretical soil mechanics. John Wiley and Sons, Inc., New York, N.Y.

VAN ZELST, T. W. 1948. An investigation of the factors affecting laboratory consolidation of clay. Proc., 2nd Int. Conf. on Soil Mechanics and Foundation Engineering, Rotterdam, Neth., vol. 7, pp. 52–61.

WALKER, L. K. and RAYMOND, G. P. 1968. The prediction of consolidation rates in a cemented clay. Can. Geot. J. **5**, pp. 192–216.